International Journal of Mass Spectrometry 302 (2011) 3–11

Contents lists available at ScienceDirect

International Journal of Mass Spectrometry

journal homepage: www.elsevier.com/locate/ijms

Hydrogen/deuterium exchange mass spectrometry and optical spectroscopy as complementary tools for studying the structure and dynamics of a membrane protein

Yan Pan[a], Leonid Brown[b], Lars Konermann[a,*]

[a] Department of Chemistry, The University of Western Ontario, London, Ontario N6A 5B7, Canada
[b] Department of Physics, University of Guelph, Guelph, Ontario N1G 2W1, Canada

ARTICLE INFO

Article history:
Received 10 March 2010
Received in revised form 17 April 2010
Accepted 21 April 2010
Available online 29 April 2010

Keywords:
Bacteriorhodopsin
Protein folding
Protein denaturation
Structural dynamics
Cell membrane

ABSTRACT

The hydrophobic nature of membrane proteins poses considerable challenges for the application of traditional analytical techniques. Hydrogen/deuterium exchange (HDX) with electrospray mass spectrometry (ESI-MS) detection is a potentially very powerful approach for investigating the structure and dynamics of membrane proteins, but thus far this technique has been applied mostly to soluble species. By using ESI-MS in conjunction with low temperature size exclusion chromatography (SEC) the current study explores the global HDX behavior of the integral membrane protein bacteriorhodopsin (BR) under various conditions. The experiments are complemented by UV–vis absorption measurements that report on the environment of the protein's retinal chromophore and fluorescence spectroscopy which probes the extent of resonance energy transfer between Trp residues and retinal. In agreement with previous reports, our HDX data imply that amide hydrogens in the transmembrane helices of native BR are highly protected, whereas most sites in solvent-exposed loops are readily exchangeable. Low temperature SEC/ESI-MS allows the labile Schiff-base linkage between protein and retinal to be completely preserved, such that the HDX properties of co-existing protein populations can be monitored individually. Solubilization of BR in sodium dodecyl sulfate (SDS) induces major structural changes and hydrolytic loss of retinal. The SDS-denatured protein appears to retain a significant degree of stable helical structure (around 25%, compared to the native state value of 74%). Bicelle-mediated refolding of SDS-denatured bacterioopsin in the presence of free retinal regenerates a native-like BR conformation with a yield close to 0.9. The HDX/SEC/ESI-MS approach developed in this work should be applicable to other membrane protein systems as well.

1. Introduction

Membrane proteins are involved in many essential processes, including oxidative phosphorylation, photosynthesis, signaling and transport. Moreover, membrane proteins represent important drug targets [1]. Despite their tremendous importance, the general understanding of membrane protein structure and function is miniscule when compared to the amount of information that is available for their water-soluble counterparts. More than 99.6% of all known protein structures are for water-soluble species [2], although roughly one third of the sequences encoded by the human genome are believed to be membrane proteins [3]. This imbalance is due to the fact that most membrane proteins are exceedingly difficult to work with. Once removed from their natural bilayer environment, they tend to undergo rapid denaturation and aggregation because of their extreme hydrophobicity. Some degree of stabilization can be achieved by embedding isolated membrane proteins in detergent micelles, bicelles (bilayered micelles) or lipid vesicles [4]. However, precipitation often still takes place in these surrogate environments. The application of traditional high resolution structure determination methods such as X-ray crystallography [5] and NMR spectroscopy [6] to membrane proteins has been demonstrated, but the success rate of these strategies is low. Alternative techniques that are capable of providing low to medium level structural information are therefore of considerable interest [7,8].

Abbreviations: AFM, atomic force microscope; BO, bacterioopsin (BR without retinal chromophore); BR, bacteriorhodopsin; CHAPS, 3-[(3-cholamidopropyl) dimethylammonio]-1-propanesulfonate; CMC, critical micelle concentration; DM, n-dodecyl-D-maltoside; DMPC, 1,2-dimyristoylphosphatidylcholine; ESI-MS, electrospray ionization mass spectrometry; FTIR, Fourier transform infrared spectroscopy; HDX, hydrogen/deuterium exchange; NMR, nuclear magnetic resonance; SDS, sodium dodecyl sulfate; SEC, size exclusion chromatography; λ_{max}, UV–vis absorption maximum.

* Corresponding author. Tel.: +1 519 661 2111x86313.
E-mail address: konerman@uwo.ca (L. Konermann).

1387-3806/$ – see front matter © 2010 Elsevier B.V. All rights reserved.
doi:10.1016/j.ijms.2010.04.011

Following its inception in the 1990s [9,10], hydrogen/deuterium exchange (HDX) in conjunction with electrospray ionization mass spectrometry (ESI-MS) has evolved into one of the most commonly used tools for probing the structure, dynamics and folding of water-soluble proteins [11–14]. Prior to that, NMR-based HDX studies had already become a well established technique [15–17]. HDX experiments rely on the fact that exposure of a protein to D_2O induces N–H → N–D conversion at backbone amide linkages. Solvent-exposed protein regions that are not involved in hydrogen bonding undergo rapid exchange, with rate constants approaching the "chemical" HDX rate constant k_{ch} of completely unprotected sites [18]. In contrast, HDX at hydrogen-bonded N–H groups is slowed down by as much as eight orders of magnitude. Exchange at these protected sites is mediated by protein structural fluctuations that involve the transient disruption of H-bonds and provide temporary solvent access [14,17]. These fluctuations may be interpreted as opening/closing events that are associated with rate constants k_{op} and k_{cl}, respectively. In the commonly encountered EX2 limit, characterized by $k_{cl} \gg k_{ch}$, the overall exchange-rate constant k_{ex} is given by $k_{ex} = (k_{op}/k_{cl}) \times k_{ch}$. Under these conditions the probability of HDX occurring during a single opening event is very small, such that numerous opening/closing cycles are required before isotope exchange takes place. Conversely, in the EX1 limit ($k_{ch} \gg k_{cl}$) exchange occurs during the very first opening event such that $k_{ex} = k_{op}$ [14,17,19]. HDX/ESI-MS is typically conducted under exchange-in conditions, where an unlabeled protein is exposed to D_2O [10,19]. Aliquots are taken at selected labeling times, followed by acid quenching at pH 2.5. The protein is then digested by pepsin or other acidic proteases [20] at 0 °C and the mass shifts of individual fragments are determined by LC/ESI-MS. In this way the HDX pattern can be uncovered in a spatially-resolved manner as a function of time [11–14]. The EX2 regime is characterized by progressive peak shifts to higher mass, whereas EX1 generally induces peak splitting [19].

Various HDX strategies have also been applied to membrane proteins. Instead of using MS detection, however, past studies in this area have largely relied on vibrational (FTIR) spectroscopy [21–23]. Upon N–H → N–D conversion the amide II band shifts from 1550 to 1450 cm^{-1}, such that global HDX information can be obtained by deconvolution of infrared spectra [24,25]. The use of ESI-MS for membrane protein HDX studies remains rare, and only a handful of studies have reported the successful application of the standard proteolytic digestion approach [26–29]. Experiments of this kind are hampered not only by solubility issues, but also by the difficulty of generating proteolytic fragments from membrane proteins in sufficiently high yield within a short time at low temperature and pH [30].

In an attempt to enhance the general applicability of HDX/ESI-MS to membrane proteins, this work explores the isotope exchange behavior of bacteriorhodopsin (BR) from *Halobacterium salinarum*. Electron microscopy [31] and X-ray crystallography [5] have revealed that the 248 residue polypeptide chain of this protein folds into seven transmembrane helices that are connected by six solvent-exposed loops, similar to the G protein-coupled receptors of higher organisms [32–34]. The seven BR helices surround a central retinal chromophore that is bound to Lys216 via a protonated Schiff-base, giving the protein its characteristic purple color. In its native environment BR is packed in clusters of three that form a two-dimensional hexagonal lattice referred to as purple membrane [31]. Trans/cis isomerization of the retinal allows the protein to act as a light-driven proton pump. The photocycle associated with this pumping process, as well as the *in vitro* folding behavior of BR has been studied extensively [5,35–38].

While the structure of native BR is well known, there continue to be uncertainties regarding the properties of this protein in environments other than the purple membrane. In particular, the structure of the SDS-denatured state continues to be a matter of debate [39,40], although this form frequently serves as starting point for BR folding experiments [41]. Using a combination of optical spectroscopy and HDX/ESI-MS, this work explores the properties of five different types of samples: BR in its native purple membrane, as well as solubilized in two different detergents (SDS and DM), refolded BR in bicelles and after cleavage of the Schiff-base linkage. Owing to the experimental difficulties outlined above, we focus on the HDX behavior of the intact protein, but it is hoped that the experiments described here set the stage for future spatially-resolved studies [26–29].

2. Materials and methods

2.1. Proteins and reagents

Purple membranes from *H. salinarum* were harvested and purified by sucrose gradient centrifugation as described previously [42–44], resulting in aqueous stock suspensions with a BR concentration of 170 μM. Samples were stored at −80 °C prior to analysis. Protein concentrations were determined for purple membrane/SDS solutions by UV–vis spectroscopy based on a molar absorption coefficient of $\varepsilon_{280} = 65{,}000\ M^{-1}\ cm^{-1}$ [45]. Deuterium oxide was obtained from Cambridge Isotope Laboratories (Andover, MA). SDS, DM, sodium phosphate, formic acid, hydroxylamine and all-*trans*-retinal were from Sigma (St. Louis, MO). DMPC was procured from Avanti (Alabaster, AL) and CHAPS from Calbiochem (San Diego, CA).

2.2. Sample preparation

To ensure consistency with previous work [46] all protein solutions were adjusted to pH 6 using 50 mM sodium phosphate buffer (referred to simply as "buffer", unless noted otherwise). Five types of different protein samples were examined. (i) For studies on native BR, purple membrane stock suspensions were prepared in buffer at a protein concentration of 100 μM. (ii) DM-solubilized protein was obtained by exposing native BR stock suspensions to 0.1% DM in buffer. These solutions were vortex-mixed for 30 s, followed by sonication in a water bath (Fisher Scientific, FS60, Ottawa, Ontario, Canada) for 15 min and equilibration at room temperature for 6 h. (iii) Bleached membranes [22,47,48] were prepared by exposing 10 μM native BR suspensions in buffer to 0.5 M hydroxylamine at pH 7.7. Subsequently the samples were irradiated for 30 h by 546 nm light from a Xe/Hg lamp, using the fiber optics-coupled output of a Biologic SFM 4S/Q (Molecular Kinetics, Indianapolis, IN) spectrometer. The resulting suspension was dialyzed twice against 3 L buffer (5 mM, pH 6) to remove hydroxylamine. The final bleached sample was lyophilized and resuspended in water to a protein concentration of 100 μM in buffer. (iv) SDS-denatured protein [40] was produced by exposing native BR stock suspension to 1.25% (w/v) SDS, followed by vortex mixing, sonication and equilibration as for the DM samples. The CMC of SDS under the conditions of this work is around 0.1% (≈3 mM) [49]. A higher concentration was used here to ensure that the detergent concentration remained well above the CMC even after dilution during HDX. (v) Refolded BR was prepared from SDS-denatured bacterioopsin (BO) following established procedures [50]. Briefly, native BR purple membranes were exposed to chloroform/methanol/triethylamine (100:100:1, v/v/v). Hydroxylamine was added to facilitate retinal removal. Addition of 0.1 M buffer in a 1:1 volume ratio followed by 10 s of vortex mixing resulted in phase separation. Delipidated BO was recovered as a precipitate at the interface. Phase separation and recovery of the protein interphase were repeated twice. The final pellet of delipidated BO was dissolved in an aqueous solution of 5% (w/v) SDS. The SDS-solubilized BO was diluted to 0.2% SDS and

dialyzed against 10 mM buffer containing 0.2% SDS for 2 days to remove residual organic solvent. To initiate refolding, the resulting delipidated BO solution in 0.2% SDS/10 mM buffer was vortex-mixed with an equal volume of buffer containing 2% DMPC/2% CHAPS bicelles at pH 6. All-*trans*-retinal (1:1 chromophore:protein molar ratio) was added simultaneously from ethanol stock. The final refolding buffer contained 1% DMPC/1% CHAPS/0.1% SDS and 0.1% ethanol. This solution was equilibrated for 1 day at room temperature in the dark.

2.3. Optical spectroscopy

UV–vis absorption measurements were carried out on a Cary 100 spectrophotometer (Varian, Mississauga, Ontario, Canada). Trp fluorescence emission spectra were acquired on a Fluorolog-3 instrument (Horiba Jobin Yvon, Edison, NJ) with an excitation wavelength of 280 nm. All optical measurements were performed at a protein concentration of 7 μM at room temperature, using protein-free solutions as blanks.

2.4. Hydrogen/deuterium exchange

Isotope exchange was initiated by mixing 100 μM protein solutions, prepared as described above, and D_2O-based buffer (with a pH meter reading of 6) at room temperature in a 1:4 volume ratio. After initiation of labeling, 35 μL aliquots were removed at various time points ranging from 1 to 120 min. These aliquots were quenched by mixing with 6 μL of 500 mM buffer (pH 2) for a final pH of 2.5, followed by flash freezing in liquid nitrogen. Zero time point controls (m_0) for the correction of artifactual in-exchange were performed by exposing protein solutions to a mixture of labeling and quenching buffer. Maximally deuterated samples (m_{100}) for the correction of back-exchange were prepared by incubating 20 μM BR in 0.4% SDS containing 80% D_2O at pH_{read} 11.8 and 40 °C for 30 h. Relative HDX levels were determined as [10]:

$$\text{Deuteration level} = \frac{m - m_0}{m_{100} - m_0} \quad (1)$$

In this expression m is the mass of the protein, and m_0 and m_{100} are the values of the corresponding control measurements. The procedure used for determining m_{100} induces retinal loss, and hence the measured mass had to be corrected by adding 284.4 Da (mass of free retinal) and subtracting 18 Da (loss of water after Schiff-base formation) for those sample that contained the chromophore. The kinetic data were fitted to the biexponential expression:

$$\text{Deuteration level} = A_1(1 - \exp[-k_1 t]) + A_2(1 - \exp[-k_2 t]) \quad (2)$$

where A_1 and A_2 are the hydrogen fractions that undergo labeling with apparent k_{ex} rate constants of k_1 and k_2, respectively.

2.5. Liquid chromatography/mass spectrometry

LC/MS measurements were conducted by using a Waters Acquity UPLC (Milford, MA) with a Waters SEC column (BioSuite, 4 μm UHR SEC, 4.6 mm × 300 mm), employing isocratic chloroform/methanol/water/formic acid (400/400/90/25, v/v/v/v) flow at 0.25 mL min^{-1} under quenching conditions (pH 2.5, 0 °C). The column and extensively coiled solvent delivery lines were embedded in an ice bath. For each injection 20 μL of sample were loaded onto the column. The protein eluted after about 10 min. The SEC column was coupled to the Z-spray ESI source of a Q-TOF Ultima API mass spectrometer (waters). Spectra were acquired in positive ion mode at a sprayer voltage of 3 kV and desolvation temperature of 250 °C. Experimental data were converted to mass distributions using the MaxEnt 1 routine provided by the instrument manufacturer for determination of m, m_0 and m_{100} in Eq. (1). Using maximally deuterated control samples, amide back-exchange was determined to be around 10%.

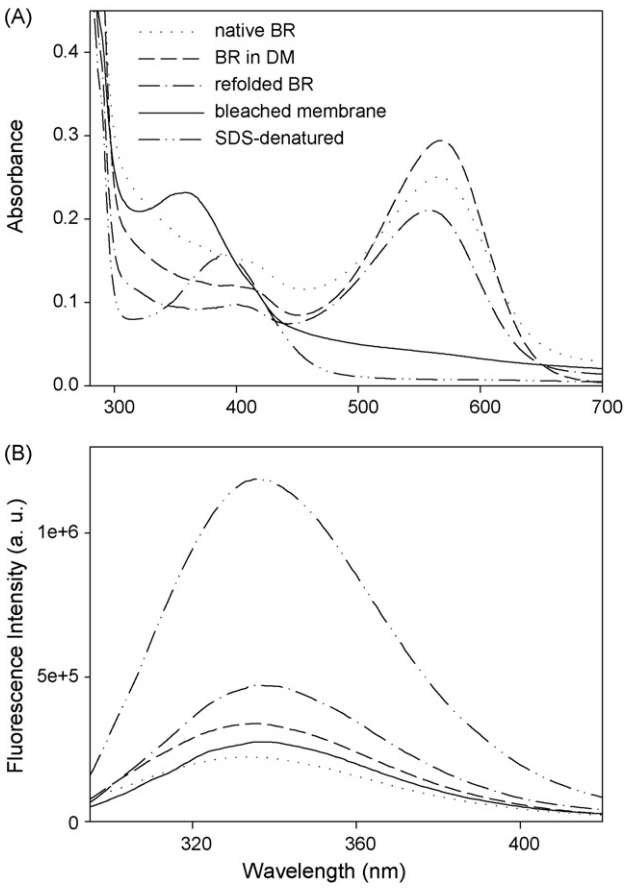

Fig. 1. (A) UV–vis absorption spectra and (B) fluorescence emission spectra of BR. The five line styles represent different experimental conditions as noted in panel A.

3. Results and discussion

3.1. Optical spectroscopy

Prior to exploring structural aspects of BR by HDX/MS, it is instructive to study the five different types of samples highlighted in this work by traditional spectroscopic tools. The retinal absorption spectrum is sensitive to the protein conformation. Native light-adapted BR in its purple membrane environment has its absorption maximum at 568 nm, indicative of the covalently linked chromophore in a structurally intact environment [51]. For the SDS-solubilized protein a maximum at 392 nm is observed (Fig. 1A). This dramatic blue shift is caused by hydrolytic cleavage of the Schiff-base linkage [40]. SDS-denaturation also affects the emission properties of the eight Trp residues [52]. Native BR exhibits a relatively low fluorescence intensity, mainly because of FRET-based retinal quenching [53] (Fig. 1B). SDS induces a 5-fold increase in Trp fluorescence intensity (Fig. 1B). These spectroscopic changes reflect the transition to a partially unfolded structure, concomitant with Schiff-base hydrolysis and release of the detergent-solubilized retinal into the solvent [54]. The lack of a major red shift in the emission reveals that SDS-denaturation does not cause significant water-exposure of Trp residues. The optical spectra obtained here for native BR and the SDS-denatured form are consistent with earlier observations [40]. The reason for including these data in Fig. 1 is to facilitate a

comparison with results obtained under the other experimental conditions.

The structural changes that occur upon solubilization of the protein are highly dependent on the detergent used. DM-solubilized BR exhibits an absorption maximum at the same wavelength as the native protein (Fig. 1A), and the fluorescence intensity increases only moderately, by a factor of less than two (Fig. 1B). This behavior is consistent with previous NMR work [55] and indicates that the DM-solubilized protein retains a structure similar to the native state, despite the breakdown of membrane-bound BR trimers into monomeric units [56]. Our data reiterate the generally accepted view of DM as a "mild" detergent that tends to preserve membrane protein structure and (to some extent) function [57–59], whereas SDS typically induces extensive structural perturbations [54].

Purple membrane bleaching by hydroxylamine entails cleavage of the retinal–protein linkage and retinaloxime formation [47], a step that is accompanied by a major change in λ_{max} to 358 nm (Fig. 1A). AFM studies have shown that this process leaves the trimeric BR structure inside the membrane largely intact, but induces loss of crystallinity [48]. Interestingly, the fluorescence emission properties of the bleached protein in Fig. 1B are almost indistinguishable from those of native BR, implying that FRET-based Trp quenching by the chromophore still takes place. It can be concluded that the detached retinaloxime remains trapped inside the chromophore binding pocket, thereby putting a qualifier on earlier suggestions of chromophore "removal" [22] under the conditions used here. Extraction of the retinaloxime from the membrane can be achieved by bovine serum albumin [60].

Exposure of SDS-denatured BO to bicelles and free retinal triggers refolding to a monomeric state [61,62]. The 557 nm absorption maximum of the refolded samples is close to that of native BR, indicating that the Schiff-base linkage between retinal and K_{216} has been regenerated for the majority of the protein molecules (Fig. 1A). Compared to the SDS-denatured state, the Trp fluorescence intensity of refolded BR is greatly reduced. However, the emission remains *ca.* 2-fold higher than for the native protein (Fig. 1B). The origin of this behavior is further investigated below.

3.2. Size exclusion chromatography/ESI-MS

With few exceptions [63,64], MS analyses of membrane proteins require the analyte to be separated from surfactants and salts. One approach is to precipitate the protein, followed by dissolution in organic solvent/acid mixtures. Alternatively, SEC or reverse-phase chromatography can be used [65]. MS studies on intact proteins are an important tool for the detection of covalently linked co-factors and post-translational modifications [66–68]. Unfortunately, the harsh solvent environment typically employed for membrane protein analyses can induce the loss of some covalently coupled moieties. For example, the MS detection of intact BR with its chromophore attached is problematic owing to the labile nature of the Schiff-base linkage. Hence, although retention of the chromophore has been demonstrated in a few instances [69,70], most previous MS studies on BR involved complete [66,71–74] or partial [75] BO formation in the course of the analysis.

During the work leading up to the HDX measurements discussed below, we initially carried out SEC/ESI-MS analyses on BR at room temperature. Those conditions resulted in partial degradation of the protein–retinal complex consistent with Ref. [75] (data not shown). It was then noticed that the stability of the complex is dramatically enhanced by lowering the elution temperature to 0 °C. Analysis of native BR under these conditions results in a major signal for the intact complex, whereas retinal-free BO is almost undetectable (Fig. 2A). Virtually the same spectrum was obtained for BR after solubilization in DM (data not shown). In contrast, SDS-denatured protein, as well as bleached membrane samples were found to be largely devoid of the covalently linked chromophore (illustrated for an SDS sample in Fig. 2B). These SEC/ESI-MS findings are in agreement with the optical results of Fig. 1, which indicated that the retinal–Lys216 bond remains intact in native and DM-solubilized BR, whereas both membrane bleaching and SDS-denaturation induce cleavage of the Schiff-base linkage.

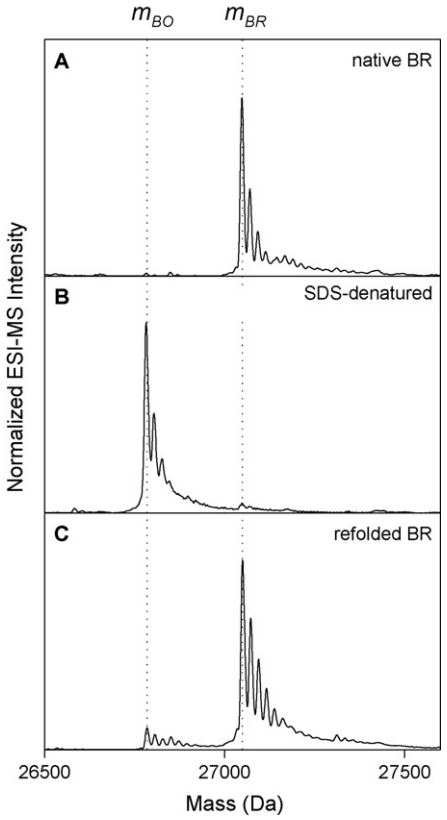

Fig. 2. Deconvoluted mass distributions obtained by SEC/ESI-MS of unlabeled protein samples at 0 °C, (A) native BR, (B) SDS-denatured state and (C) refolded BR. Satellite peaks are due to sodium adducts. Dashed vertical lines indicate the masses expected for BO (m_{BO} = 26,784 Da) [66] and BR (m_{BR} = 27,050 Da) [75].

From the data of Fig. 2A and B it can be concluded that the low temperature SEC/ESI-MS procedure used here provides an accurate reflection of the retinal binding state in bulk solution. This technique can therefore be used to determine the regeneration yield of samples that had undergone SDS-denaturation and subsequent refolding. Typical SEC/ESI-MS data for refolded BR are depicted in Fig. 2C, revealing the presence of a dominant peak for the retinal-bound protein and a less intense signal for BO. On the basis of the 8:1 peak intensity ratio the regeneration yield is 8/9 = 89%, which is in close agreement with the A_{568} ratio of the two samples in Fig. 1A, as well as with previously reported values [50]. The presence of 11% BO after refolding contributes to the elevated fluorescence intensity in Fig. 1B (dash-dotted line).

3.3. Hydrogen/deuterium exchange SEC/ESI-MS

HDX/ESI-MS protocols typically employ reverse-phase chromatography [76]. For the membrane protein experiments of this work we pursued the SEC-based strategy outlined above, as it allows the covalently linked chromophore to be preserved during analysis, such that co-existing BO and BR species in solution can be monitored separately.

High quality intact protein HDX data were obtained for all five experimental conditions. Native BR undergoes only a relatively small mass change during the 120 min time window examined here

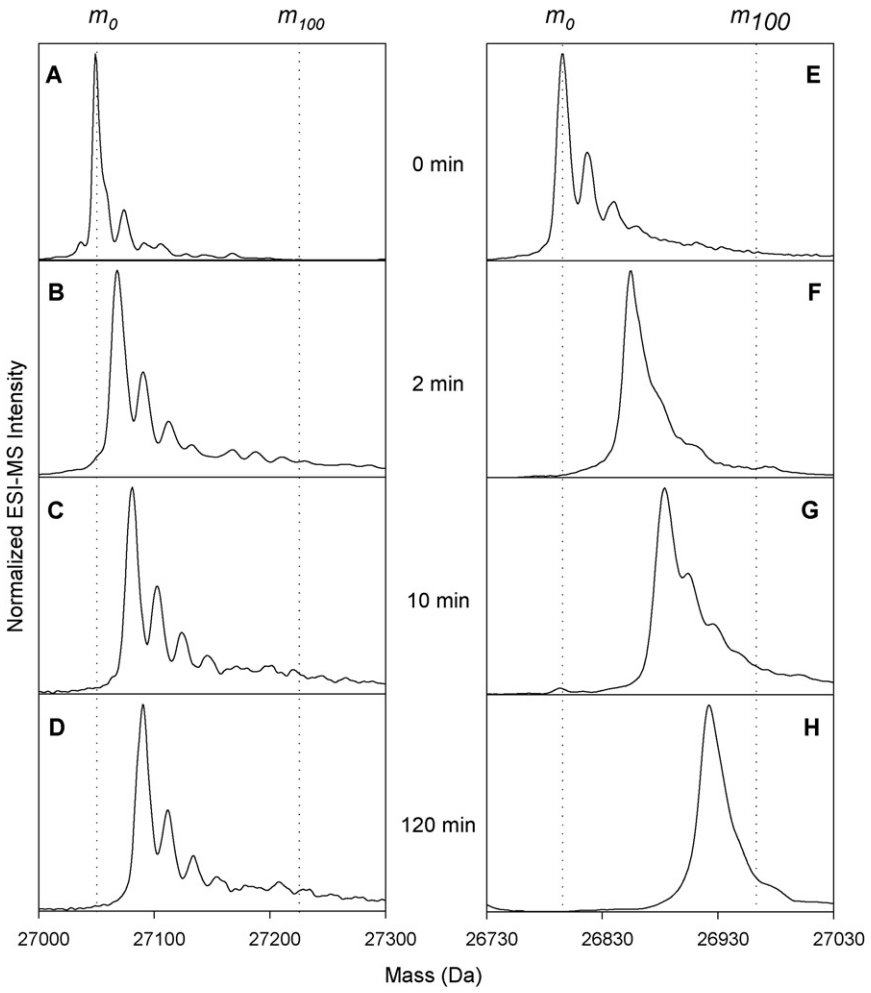

Fig. 3. Deconvoluted ESI mass distributions of native BR (A–D) and SDS-denatured protein (E–H), obtained after HDX for exchange times of $t = 0$, 2, 10 and 120 min. Dotted lines represent mass values for the m_0 and m_{100} controls. The mass range for the SDS samples (panels on the right hand side) is shifted to account for the loss of retinal.

(Fig. 3A–D). In contrast, much more extensive HDX is observed for the SDS-denatured state (Fig. 3E–H). All the samples studied in this work underwent gradual mass shifts without peak splitting, indicative of HDX in the EX2 regime [19]. Satellite peaks in Fig. 3 are due to sodium adducts, not to EX1 dynamics.

Amide deuteration levels were determined according to Eq. (1) (Fig. 4). The HDX kinetics were analysed on the basis of a biphasic expression (Eq. (2)), resulting in fits that are shown as solid lines in Fig. 4 (parameters are summarized in Table 1). The apparent rate constants determined by this approach are on the order of $k_1 \approx 1\,\text{min}^{-1}$ and $k_2 \approx 0.1\,\text{min}^{-1}$. The kinetic amplitudes associated with these two phases represent the percentage of amide hydrogens that are weakly (A_1) and moderately protected (A_2). $A_{\text{non-ex}} = 100 - A_1 - A_2$ represents the percentage of amide hydrogens that is non-exchangeable on the time scale of our experiments.

Table 1
Parameters obtained from fitting the HDX kinetics of Fig. 4A according to the biexponential expression of Eq. (2). The percentage of "non-exchangeable" hydrogens (last column) has been calculated as $A_{\text{non-ex}} = 100 - A_1 - A_2$.

	A_1 (%)	k_1 (min^{-1})	A_2 (%)	k_2 (min^{-1})	$A_{\text{non-ex}}$ (%)
Native BR	12.0	1.5	11.7	0.074	76.3
BR in DM	16.6	1.5	9.7	0.074	73.7
Refolded BR	26.9	0.97	10.7	0.027	62.4
Bleached membrane	21.5	2.1	11.9	0.050	66.6
SDS-denatured	46.7	0.69	28.5	0.028	24.8

In the case of native BR, $A_1 = 12\%$ of the amide hydrogens are weakly protected, $A_2 = 11.7\%$ are moderately protected and $A_{\text{non-ex}} = 76.3\%$ do not undergo exchange (Table 1). It is interesting to compare these data with the H-bonding pattern in the 1.55 Å X-ray structure of the protein. Stable H-bonds were identified by analyzing pdb file 1C3W [5] using Swiss PDB Viewer default values [77] i.e., a donor–acceptor distance between 2.195 and 3.3 Å, respectively and a minimum angle of 90°. According to this analysis, almost all of the amide N–H groups in the transmembrane helices are H-bonded, with the exception of a small number of residues close to the helix termini. Most of the non-bonded N–H groups are located in the extramembrane loops (Table 2). BR has a total of 248 residues, corresponding to 247 backbone amide bonds. Taking into account the presence of 11 prolines, the number of backbone N–H groups is 236. Table 2 shows 181 stable H-bonds, which means that an amide fraction of 181/236 = 76.7% is expected to be strongly protected. This value is in very close agreement with the measured value of $A_{\text{non-ex}} = 76.3\%$. A high resilience against HDX in the seven transmembrane helices has previously been inferred from tritium exchange [78,79] and infrared spectroscopic HDX studies [21,23], which found the total amide protection to be in the range of 71–80%. Our HDX kinetics show that the remaining N–H groups in native BR can be grouped in two categories. $A_2 = 11.7\%$ are likely involved in weak hydrogen bonds that do not appear in the X-ray structure when applying the criteria listed above. The remaining $A_1 = 12\%$ experience an even lower degree of protection, although their apparent rate constant ($k_1 = 1.5\,\text{min}^{-1}$) is below the value

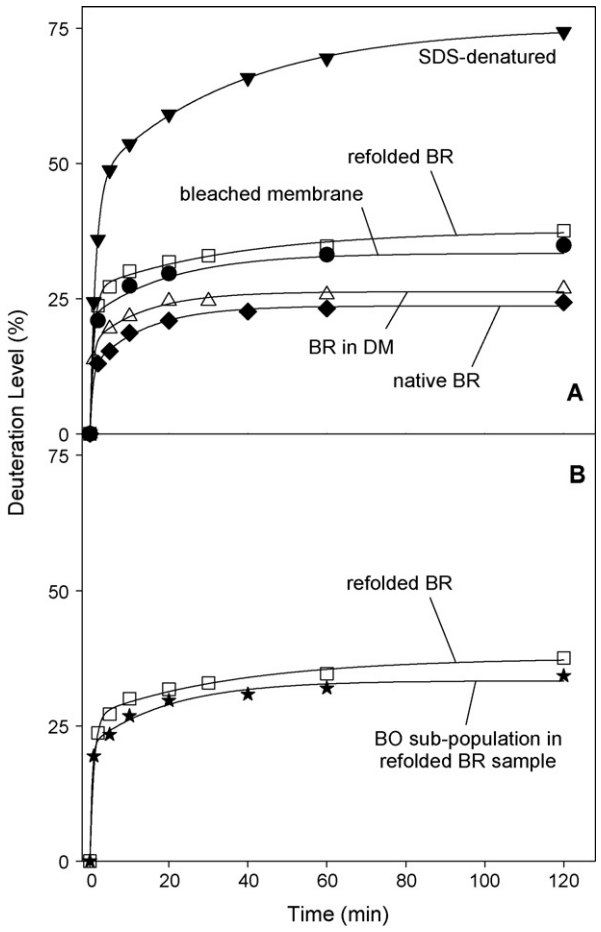

Fig. 4. (A) HDX kinetics of BR under five different solvent conditions, normalized according to Eq. (1). Each data point represents an average of two or three independent measurements. The experimental error was found to be less than 2%. Solid lines are biexponential fits, using the expression of Eq. (2). Fitting parameters are summarized in Table 1. (B) Refolded BR data (open squares) are identical to those in panel A. Star-shaped symbols represent the HDX behavior of the 11% BO sub-population in the refolded BR sample (see Fig. 2C).

of $k_{ch} \approx 60\,min^{-1}$ that would be expected for completely exposed amides in a random coil environment [18].

Solubilization of BR in SDS results in dramatically more extensive HDX. Almost half of all amide hydrogens become rapidly exchangeable ($A_1 = 46.7\%$), whereas $A_2 = 28.5\%$ undergo isotope exchange with an apparent rate constant of $k_2 = 0.028\,min^{-1}$. Only one quarter ($A_{non\text{-}ex} = 24.8\%$) of all amide hydrogens are non-exchangeable in SDS. These HDX kinetics suggest partial helix unravelling in the SDS state as proposed earlier [39,46], but with retention of a protein core that remains inaccessible to solvent water [40]. Our findings reveal that this residual core encompasses a total of $0.248 \times 236 \approx 59$ protected backbone amides.

In contrast to the behavior observed after SDS exposure, solubilization of BR in DM results in HDX kinetics that are almost indistinguishable from those of the native state (Fig. 4, Table 1). Hence, the transition from the native trimeric structure in the purple membrane to a monomeric DM-solubilized state [56] induces virtually no changes to the BR structure and dynamics, as previously suggested on the basis of NMR data [55].

Bleached membranes exhibit a roughly 2-fold increase in the amplitude of rapidly exchanging hydrogens (A_1) relative to native BR, whereas the value of A_2 remains more or less unchanged. Comparison with the HDX behavior of the SDS-denatured state shows that the structural perturbations induced by cleavage of the Schiff-base are relatively moderate. The percentage of non-exchangeable amide hydrogens in the bleached membranes is 66.6%. Our findings are consistent with previous ^{13}C-NMR [47,80], AFM [48], FRET [81] and infrared studies [22], all of which indicate that the protein structure in the bleached membrane remains similar to that of native BR, despite the loss of membrane crystallinity and the occurrence of greater disorder in some local regions. Thus, major aspects of the native BR structure are not dependent on the presence of an intact covalent linkage between protein and chromophore.

As noted in Section 1, one intriguing feature of BR is the possibility to refold the protein in a bicelle environment after SDS-denaturation [41,45]. In contrast to the crystalline trimeric assembly within the purple membrane, refolded BR is monomeric [61,62]. It remains somewhat unclear in how far individual refolded protein chains differ from the native structure in terms of their structure and dynamics. Optical assays of the type discussed above (Fig. 1) are not necessarily suitable for exploring this interesting question, because the spectra represent ensemble averages. In particular, it is difficult to decide whether the presence of 11% BO in the refolded samples (Fig. 2C) can account for the elevated fluorescence intensity seen in Fig. 1B, and whether the 89% BR population is affected by structural perturbations. The SEC/ESI-MS protocol employed here allows the HDX behavior of BO and BR in the refolded samples to be monitored separately. We find that the HDX kinetics of these two co-existing sub-population are very similar to each other (Fig. 4B), resembling the behavior seen for bleached membranes (Fig. 4A). Thus, it can be concluded that *in vitro* refolding of the protein leads to a native-like conformation,

Table 2
Amino acid sequence of BR [90]. Residues that act as amide N–H hydrogen bond donor (to an amide carbonyl, or to a side chain acceptor) are underlined and bold. Hydrogen bonds were determined from the X-ray structure of native BR [5] using the procedure outlined in the text. Non-hydrogen-bonded residues include 11 prolines, as well as three short disordered segments (italicized, not seen in the X-ray structure [5]). X represents pyroglutamate [66].

Segment	Sequence	H-bonds
N-term.	^{1}*X A Q I* T G **R** P^{8}	1
Helix A	^{9}E **W** I **W L A L G T A L M G L G T L Y F L V K G**^{31}	21
A–B loop	^{32}**M G V** S^{35}	3
Helix B	^{36}D P D **A K K F Y A I T T L V** P **A I A F T M Y L S M L L G**^{63}	24
B–C loop	^{64}**Y G** L **T** M **V** P **F** G G **E** Q **N** P I Y **W**^{80}	9
Helix C	^{81}**A** R **Y A D W L F T T** P **L L L L D L A L L V**^{101}	19
C–D loop	^{102}**D A**^{103}	2
Helix D	^{104}D Q G **T I L A L V G A D G I M I G T G L V G A L**^{127}	21
D–E loop	^{128}**T** K V Y S^{132}	1
Helix E	^{133}**Y R F V W W A I S T A A M L Y I L Y V L F F G**^{155}	23
E–F loop	^{156}F *T S K A E* S M^{163}	0
Helix F	^{164}R P E **V A S T F K V L R N V T V V L W S A Y** P **V V W L I G**^{92}	25
F–G loop	^{193}**S** E **G A G I V**^{199}	6
Helix G	^{200}P L N **I E T L L F M V L D V S A K V G F G L I L L R**^{225}	23
C-term.	^{226}**S** R **A** I **F** G *E A E A P E P S A G D G A A A T S*^{248}	3

but that structural perturbations persist for both the retinal-bound (89%) and the retinal-free (11%) forms. NMR data suggest that some of this disorder is attributable to loop elements that do not fully recover during BR folding *in vitro* [80,82]. Our findings suggest that the chromophore plays a relatively minor role in guiding the protein along its folding pathway, at least as far as the formation of secondary structure is concerned [83]. This assertion is in agreement with recent oxidative labeling experiments, which revealed that the retinal-free protein can fold into a conformation resembling the native state, where only one of the seven helices (D) remains partially disordered [40].

4. Conclusions

This work employed a combination of optical spectroscopy and ESI-MS-based methods for exploring the structure and dynamics of BR under various experimental conditions. UV–vis absorption measurements report on the intactness of the Schiff-base linkage between protein and retinal, whereas the fluorescence intensity is sensitive to changes in retinal–tryptophan distance. Low temperature SEC/ESI-MS was found to be an even more direct tool for probing the intactness of the sensitive Schiff-base linkage. This procedure will likely be applicable to other retinal-containing membrane proteins as well. SDS-denaturation and purple membrane bleaching induce loss of the chromophore, whereas solubilization in DM leaves the linkage intact. Bicelle-mediated refolding predominantly results in the formation of BR, whereas a smaller fraction of the protein remains in the BO state. HDX measurements by SEC/ESI-MS were shown to represent a straightforward alternative to traditional infrared spectroscopy experiments [21–23] for monitoring global changes in BR structure and dynamics. To the best of our knowledge, this study conducts the first side-by-side comparison of the HDX characteristics for this important model system under different biochemical conditions. Backbone amide hydrogens within the seven transmembrane helices of native BR are highly protected. The number of non-exchangeable hydrogens decreases in the order native BR ≈ DM-solubilized BR > bleached membranes ≈ refolded BO ≈ refolded BR ≫ SDS-denatured state. However, even the SDS-denatured protein retains a sizeable number of protected backbone amides. This finding is consistent with recent covalent labeling data that found the SDS-solubilized state to be only partially unfolded, with a core that remains inaccessible to the solvent [40].

On the basis of CD measurements it has previously been suggested that SDS-denaturation reduces the helical content of the protein from the native state value of 74% down to 42% [46]. That interpretation has subsequently been challenged by noting that CD studies on BR are associated with unique experimental difficulties [39]. It is interesting to compare those previous CD data to the findings of the current work. When judging the secondary structure content of the SDS state on the basis of amide protection, our data suggest that $A_{\text{non-ex}} = 24.8\%$ of all amide hydrogens are involved in stable helical elements (Table 2). In addition, the $A_2 = 28.5\%$ moderately protected hydrogens in SDS are likely located in regions that retain some helix propensity as well. A residual helicity of 42% in SDS as suggested in Ref. [46] is therefore not in disagreement with our findings. It is noted, however, that caution should be exercised when estimating the secondary structure content of a membrane protein solely on the basis of HDX data, because amide protection might involve significant contributions from solvent shielding by the surrounding surfactant molecules [8].

Although this work provides interesting information on the global structure and dynamics of BR, the lack of a robust protocol for spatially-resolved membrane protein studies represents a severe impediment for studies in this area. In a recent study, Joh et al. applied the traditional proteolytic digestion/LC/MS approach to BR [28]. Focusing exclusively on the SDS-denatured state, those authors obtained limited coverage (five regions covering less than half of the protein sequence). Spatially-resolved data for native BR could not be obtained [28]. Unfortunately, we were not successful in extending the approach of that work further, neither by using pepsinolysis in bulk solution, nor by employing a pepsin column. We attribute these difficulties to the well known tendency of BR to precipitate under the acidic conditions required for HDX quenching [84]. Rietschel et al. [30] recently reported the successful pepsinolysis of BR, but only under conditions that are incompatible with the HDX workflow, i.e., up to 16 h of digestion at room temperature. Nonetheless, results obtained for a number of other systems [26,27,29] suggest that spatially-resolved HDX/ESI-MS studies on membrane proteins will soon cease to be considered a fringe area. We are confident that that this development will be spurred by ongoing improvements of the HDX and digestion workflow [85–87], possibly in combination with the application of electron-based dissociation techniques [88,89].

Acknowledgements

This work was supported by the Natural Sciences and Engineering Research Council of Canada (NSERC), the Canada Foundation for Innovation (CFI), the Canada Research Chairs Program, and The University of Western Ontario. Fluorescence measurements were carried out at the UWO Biomolecular Interactions and Conformations Facility which is supported by the Schulich School of Medicine & Dentistry.

References

[1] S.R. George, B.F. O'Dowd, S.P. Lee, G-protein-coupled receptor oligomerization and its potential for drug discovery, Nat. Rev. Drug Discov. 1 (2002) 808–820.
[2] S.H. White, Biophysical dissection of membrane proteins, Nature 459 (2009) 344–346.
[3] C.C. Wu, J.R. Yates III, The application of mass spectrometry to membrane proteins, Nat. Biotechnol. 21 (2003) 262–267.
[4] C.R. Sanders, R.S. Prosser, Bicelles: a model membrane system for all seasons? Structure 6 (1998) 1227–1234.
[5] H. Luecke, B. Schobert, H. Richter, J. Cartailler, J.K. Lanyi, Structure of bacteriorhodopsin at 1.55 A resolution, J. Mol. Biol. 291 (1999) 899–911.
[6] A. Arora, F. Abilgaard, J.H. Bushweller, L.K. Tamm, Structure of outer membrane protein A transmembrane domain by NMR spectroscopy, Nat. Struct. Biol. 8 (2001) 334–338.
[7] A.B. Weinglass, Probing the structure and function of integral membrane proteins by mass spectrometry, in: J.P. Whitelegge (Ed.), Protein Mass Spectrometry, Elsevier, Amsterdam, 2009, pp. 197–212.
[8] Y. Pan, L. Konermann, Membrane protein structural insights from chemical labeling and mass spectrometry, Analyst (2010), doi:10.1039/b924805f, in press.
[9] V. Katta, B.T. Chait, Conformational changes in proteins probed by hydrogen-exchange electrospray-ionisation mass spectrometry, Rapid Commun. Mass Spectrom. 5 (1991) 214–217.
[10] D.L. Smith, Y. Deng, Z. Zhang, Probing the noncovalent structure of proteins by amide hydrogen exchange mass spectrometry, J. Mass Spectrom. 32 (1997) 135–146.
[11] J.R. Engen, Analysis of protein conformation and dynamics by hydrogen/deuterium exchange MS, Anal. Chem. 81 (2009) 7870–7875.
[12] S.W. Englander, Hydrogen exchange and mass spectrometry: a historical perspective, J. Am. Soc. Mass Spectrom. 17 (2006) 1481–1489.
[13] C.S. Maier, M.L. Deinzer, Protein conformations, interactions, and H/D exchange, Methods Enzymol. 402 (2005) 312–360.
[14] S.J. Eyles, I.A. Kaltashov, Methods to study protein dynamics and folding by mass spectrometry, Methods 34 (2004) 88–99.
[15] F.M. Hughson, P.E. Wright, R.L. Baldwin, Structural characterisation of a partly folded apomyoglobin intermediate, Science 249 (1990) 1544–1548.
[16] K.S. Kim, J.A. Fuchs, C.K. Woodward, Hydrogen exchange identifies native state motional domains important in protein folding, Biochemistry 32 (1993) 9600–9608.
[17] M.M.G. Krishna, L. Hoang, Y. Lin, S.W. Englander, Hydrogen exchange methods to study protein folding, Methods 34 (2004) 51–64.
[18] Y. Bai, J.S. Milne, L. Mayne, S.W. Englander, Primary structure effects on peptide group hydrogen exchange, Proteins Struct. Funct. Genet. 17 (1993) 75–86.
[19] L. Konermann, X. Tong, Y. Pan, Protein structure and dynamics studied by mass spectrometry: H/D exchange, hydroxyl radical labeling, and related approaches, J. Mass Spectrom. 43 (2008) 1021–1036.

[20] M. Rey, P. Man, G. Brandolin, E. Forest, L. Pelosi, Recombinant immobilized rhizopuspepsin as a new tool for protein digestion in hydrogen/deuterium exchange mass spectrometry, Rapid Commun. Mass Spectrom. 23 (2009) 3431–3438.
[21] T.N. Earnest, J. Herzfeld, K.J. Rothschild, Polarized fourier transform infrared spectroscopy of bacteriorhodopsin. Transmembrane alpha helices are resistant to hydrogen/deuterium exchange, Biophys. J. 58 (1990) 1539–1546.
[22] J. Cladera, J. Torres, E. Padros, Analysis of conformational changes in bacteriorhodopsin upon retinal removal, Biophys. J. 70 (1996) 2882–2887.
[23] N.W. Downer, T.J. Bruchman, J.H. Hazzard, Infrared spectroscopic study of photoreceptor membrane and purple membrane. Protein secondary structure and hydrogen deuterium exchange, J. Biol. Chem. 261 (1986) 3640–3647.
[24] A. Barth, Infrared spectroscopy of proteins, Biochim. Biophys. Acta 1767 (2007) 1073–1101.
[25] H. Laczko-Dobos, B. Szalontai, Lipids, proteins, and their interplay in the dynamics of temperature-stressed membranes of a cyanobacterium, synechocystis PCC 6803, Biochemistry 48 (2009) 10120–10128.
[26] L.S. Busenlehner, S.G. Codreanu, P.J. Holm, P. Bhakat, H. Hebert, R. Morgenstern, R.N. Armstrong, Stress sensor triggers conformational response of the integral membrane protein microsomal glutathione transferase 1, Biochemistry 43 (2004) 11145–11152.
[27] L.S. Busenlehner, L. Salomonsson, P. Brzezinski, R.N. Armstrong, Mapping protein dynamics in catalytic intermediates of the redox-driven proton pump cytochrome c oxidase, Proc. Natl. Acad. Sci. U.S.A. 103 (2006) 15398–15403.
[28] N.H. Joh, A. Min, S. Faham, J.P. Whitelegge, D. Yang, V.L. Woods, J.U. Bowie, Modest stabilization by most hydrogen-bonded side-chain interactions in membrane proteins, Nature 453 (2008) 1266–1270.
[29] X. Zhang, E.Y.T. Chien, M.J. Chalmers, B.D. Pascal, J. Gatchalian, R.C. Stevens, P.R. Griffin, Dynamics of the ß2-adrenergic G-protein coupled receptor revealed by hydrogen–deuterium exchange, Anal. Chem. 82 (2010) 1100–1108.
[30] B. Rietschel, S. Bornemann, T.N. Arrey, D. Baeumlisberger, M. Karas, B. Meyer, Membrane protein analysis using an improved peptic in-solution digestion protocol, Proteomics 9 (2009) 5553–5557.
[31] R. Henderson, P.N. Unwin, Three-dimensional model of purple membrane structure obtained by electron microscopy, Nature 257 (1975) 28–32.
[32] K. Palczewski, T. Kumasaka, T. Hori, C.A. Behnke, H. Motoshima, B.A. Fox, I.L. Trong, D.C. Teller, T. Okada, R.E. Stenkamp, M. Yamamoto, M. Miyano, Crystal structure of rhodopsin: a G protein-coupled receptor, Science 289 (2000) 739–745.
[33] V. Cherezov, D.M. Rosenbaum, M.A. Hanson, S.G.F. Rasmussen, F.S. Thian, T.S. Kobilka, H. Choi, P. Kuhn, W.I. Weis, B.K. Kobilka, R.C. Stevens, High-resolution crystal structure of an engineered human β2-adrenergic G protein-coupled receptor, Science 318 (2007) 1258–1265.
[34] V.-P. Jaakola, M.T. Griffith, M.A. Hanson, V. Cherezov, E.Y.T. Chien, J.R. Lane, A.P. Ijzerman, R.C. Stevens, The 2.6 Angstrom crystal structure of a human A2A adenosine receptor bound to an antagonist, Science 322 (2008) 1211–1217.
[35] U. Haupts, J. Tittor, D. Oesterhelt, Closing in on bacteriorhodopsin: progress in understanding the molecule, Annu. Rev. Biophys. Biomol. Struct. 28 (1999) 367–399.
[36] J. Heberle, J. Fitter, H.J. Sass, G. Büldt, Bacteriorhodopsin: the functional details of a molecular machine are being resolved, Biophys. Chem. 85 (2000) 229–248.
[37] S. Subramaniam, T. Hirai, R. Henderson, From structure to mechanism: electron crystallographic studies of bacteriorhodopsin, Philos. Trans. R. Soc. Lond. A 360 (2002) 859–874.
[38] R.R. Birge, N.B. Gillespie, E.W. Izaguirre, A. Kusnetzow, A.F. Lawrence, D. Singh, W. Song, E. Schmidt, J.A. Stuart, S. Seetharaman, K.J. Wise, Biomolecular, Electronics:, Protein-based associative processors and volumetric memories, J. Phys. Chem. B 103 (1999) 10746–10766.
[39] R. Renthal, An unfolding story of helical transmembrane proteins, Biochemistry 45 (2006) 14559–14566.
[40] Y. Pan, L. Brown, L. Konermann, Mapping the structure of an integral membrane protein under semi-denaturing conditions by laser-induced oxidative labeling and mass spectrometry, J. Mol. Biol. 394 (2009) 968–981.
[41] P. Curnow, P.J. Booth, The transition state for integral membrane protein folding, Proc. Natl. Acad. Sci. U.S.A. 106 (2009) 773–778.
[42] B. Ni, M. Chang, A. Duschl, J. Lanyi, R. Needleman, An efficient system for the synthesis of bacteriorhodopsin in halobacterium halobium, Gene 90 (1990) 169–172.
[43] Y. Pan, B.B. Stocks, L. Brown, L. Konermann, Structural characterization of an integral membrane protein in its natural lipid environment by oxidative methionine labeling and mass spectrometry, Anal. Chem. 81 (2009) 28–35.
[44] D. Oesterhelt, W. Stoeckenius, Isolation of the cell membrane of halobacterium halobium and its fractionation into red and purple membrane, Methods Enzymol. 31 (1974) 667–678.
[45] K. Huang, H. Bayley, M. Liao, E. London, H.G. Khorana, Refolding of an integral membrane protein, J. Biol. Chem. 256 (1981) 3802–3809.
[46] M.L. Riley, B.A. Wallace, S.L. Flitsch, P.J. Booth, Slow α helix formation during folding of a membrane protein, Biochemistry 36 (1997) 192–196.
[47] S. Yamaguchi, S. Tuzi, M. Tanio, A. Naito, J.K. Lanyi, R. Needleman, H. Saitio, Irreversible conformational change of bacteriorhodopsin induced by binding of retinal during its reconstitution to bacteriorhodopsin, as studied by ^{13}C NMR, J. Biochem. 127 (2000) 861–869.
[48] C. Möller, G. Büldt, N.A. Dencher, A. Engel, D.J. Müller, Reversible loss of crystallinity on photobleaching purple membrane in the presence of hydroxylamine, J. Mol. Biol. 301 (2000) 869–879.
[49] J.C. Jacquier, P.L. Desbene, Determination of critical micelle concentration by capillary electrophoresis. Application to organo-saline electrolytes, J. Chromatogr. A 743 (1996) 307–314.
[50] P.J. Booth, A. Farooq, S.L. Flitsch, Retinal binding during folding and assembly of the membrane protein bacteriorhodopsin, Biochemistry 35 (1996) 5902–5909.
[51] J. Wang, C.D. Heyes, M.A. El-Sayed, Refolding of thermally denatured bacteriorhodopsin in purple membrane, J. Phys. Chem. 106 (2002) 723–729.
[52] Y. Chen, M.D. Barkley, Toward understanding tryptophan fluorescence in proteins, Biochemistry 37 (1998) 9976–9982.
[53] O. Kalisky, J. Feitelson, M. Ottolenghi, Photochemistry and fluorescence of bacteriorhodopsin excited in its 280 nm absorption band, Biochemistry 20 (1981) 203–209.
[54] C. Michaux, N.C. Pomroy, G.G. Prive, Refolding SDS-denatured proteins by the addition of amphipathic cosolvents, J. Mol. Biol. 375 (2008) 1477–1488.
[55] H. Patzelt, S.D. Ulrich, H. Egbringhoff, P. Dux, J. Ashurst, B. Simon, H. Oschkinat, D. Oesterhelt, Towards structural investigations on isotope labelled native bacteriorhodopsin in detergent micelles by solution-state NMR spectroscopy, J. Biomol. NMR 10 (1997) 95–106.
[56] M. Seigneuret, J.-M. Neumann, J.-L. Rigaut, Detergent Delipidation and solubilization strategies for high-resolution NMR of the membrane protein bacteriorhodopsin, J. Biol. Chem. 266 (1991) 10066–10069.
[57] R.M. Garavito, S. Ferguson-Miller, Detergents as tools in membrane biochemistry, J. Biol. Chem. 276 (2001) 32403–32406.
[58] M. le Maire, P. Champeil, J.V. Moller, Interaction of membrane proteins and lipids with solubilizing detergents, Biochim. Biophys. Acta 1508 (2000) 86–111.
[59] L. Qin, C. Hiser, A. Mulichak, R.M. Garavito, S. Ferguson-Miller, Identification of Conserved lipid/detergent-binding sites in a high-resolution structure of the membrane protein cytochrome c oxidase, Proc. Natl. Acad. Sci. U.S.A. 103 (2006) 16117–16122.
[60] G. Büldt, K. Konno, K. Nakanishi, H.-J. Plöhn, B.N. Rao, N.A. Dencher, Heavy-atom labelled retinal analogues located in bacteriorhodopsin by X-ray diffraction, Photochem. Photobiol. 54 (1991) 873–879.
[61] C.G. Brouillette, R.B. Mcmichens, L.J. Stern, H.G. Khorana, Structure and thermal stability of monomeric bacteriorhodopsin in mixed phospholipid/detergent micelles, Proteins Struct. Funct. Genet. 5 (1989) 38–46.
[62] S. Faham, J.U. Bowie, Bicelle crystallization: a new method for crystallizing membrane proteins yields a monomeric bacteriorhodopsin structure, J. Mol. Biol. 316 (2002) 1–6.
[63] N.P. Barrera, N. Di Bartolo, P.J. Booth, C.V. Robinson, Micelles protect membrane complexes from solution to vacuum, Science 321 (2008) 243–246.
[64] W. Stelzer, B.C. Poschner, H. Stalz, A.J. Heck, D. Langosch, Sequence-specific conformational flexibility of SNARE transmembrane helices probed by hydrogen/deuterium exchange, Biophys. J. 95 (2008) 1326–1335.
[65] J.P. Whitelegge, Intact protein mass measurements and top-down mass spectrometry: application to integral membrane proteins, in: J.P. Whitelegge (Ed.), Protein Mass Spectrometry, Elsevier, Amsterdam, 2009, pp. 179–196.
[66] P. Hufnagel, U. Schweiger, C. Eckerskorn, D. Oesterhelt, Electrospray ionization mass spectrometry of genetically and chemically modified bacteriorhodopsin, Anal. Biochem. 243 (1996) 46–54.
[67] J.P. Whitelegge, J. Le Coutre, J.C. Lee, C.K. Engel, G.G. Prive, K.F. Faull, H.R. Kaback, Toward the bilayer proteome, electrospray ionization-mass spectrometry of large, intact transmembrane proteins, Proc. Natl. Acad. Sci. U.S.A. 96 (1999) 10695–10698.
[68] N. Siuti, N.L. Kelleher, Decoding protein modifications using top-down mass spectrometry, Nat. Methods 4 (2007) 817–821.
[69] J.P. Whitelegge, C.B. Gundersen, K.F. Faull, Electrospray-ionization mass spectrometry of intact intrinsic membrane proteins, Protein Sci. 7 (1998) 1423–1430.
[70] K.L. Schey, D.I. Papac, D.R. Knapp, R.K. Crouch, Matrix-assisted laser desorption mass spectrometry of rhodopsin and bacteriorhodopsin, Biophys. J. 63 (1992) 1240–1243.
[71] J. Schaller, B.C. Pellascio, U.P. Schlunegger, analysis of hydrophobic proteins and peptides by electrospray ionization mass spectrometry, Rapid Commun. Mass Spectrom. 11 (1997) 418–426.
[72] J. Whitelegge, Tandem mass spectrometry of integral membrane proteins for top-down proteomics, Trends Anal. Chem. 24 (2005) 576–582.
[73] D.R. Barnidge, E. Dratz, A.J. Jesaitis, J. Sunner, Extraction method for analysis of detergent-solubilized bacteriorhodopsin and hydrophobic peptides by electrospray ionization mass spectrometry, Anal. Biochem. 269 (1999) 1–9.
[74] P.A. Schindler, A. Vandorsselaer, A.M. Falick, Analysis of hydrophobic proteins and peptides by electrospray ionization mass spectrometry, Anal. Biochem. 213 (1993) 256–263.
[75] J.P. Whitelegge, F. Halgand, P. Souda, V. Zabrouskov, Top-down mass spectrometry of integral membrane proteins, Exp. Rev. Proteomics 3 (2006) 585–596.
[76] T.E. Wales, J.R. Engen, Hydrogen exchange mass spectrometry for the analysis of protein dynamics, Mass Spectrom. Rev. 25 (2006) 158–170.
[77] N. Guex, M.C. Peitsch, Swiss-model and the Swiss-Pdb viewer: an environment for comparative protein modeling, Electrophoresis 18 (1997) 2714–2723.
[78] T. Konishi, L. Packer, Hydrogen exchange of dark-adapted and illuminated bacteriorhodopsin, FEBS Lett. 80 (1977) 455–458.
[79] J.J. Englander, S.W. Englander, Comparison of bacterial and animal rhodopsins by hydrogen exchange studies, Nature 265 (1977) 658–659.
[80] I. Kawamura, J. Tanabe, M. Ohmine, S. Yamaguchi, S. Tuzi, A. Naito, Participation of the BC loop in the correct folding of bacteriorhodopsin as revealed by solid-state NMR, Photochem. Photobiol. 85 (2009) 624–630.

[81] S.J. Nannepaga, R. Gawalapu, D. Velasquez, R. Renthal, Estimation of helix–helix association free energy from partial unfolding of bacterioopsin, Biochemistry 43 (2004) 550–559.
[82] M. Tanio, S. Tuzi, S. Yamaguchi, H. Konishi, A. Naito, R. Needleman, J.K. Lanyi, H. Saitô, Evidence of local conformational fluctuations and changes in bacteriorhodopsin, dependent on lipids, detergents and trimeric structure, as studied by ^{13}C NMR, Biochim. Biophys. Acta 1375 (1998) 84–92.
[83] P.J. Booth, S.L. Fitsch, L.J. Stern, D.A. Greenhalgh, P.S. Kim, H.G. Khorana, Intermediates in the folding of the membrane protein bacteriorhodopsin, Nat. Struct. Biol. 2 (1995) 139–143.
[84] P.C. Mowery, R. Lozier, H.Q. Chae, G.C. Tseng, M. Taylor, W. Stoeckenius, Effect of acid pH on the absorption spectra and photoreactions of bacteriorhodopsin, Biochemistry 18 (1979) 4100–4107.
[85] H.M. Zhang, S.M. McLoughlin, S.D. Frausto, H.L. Tang, M.R. Emmett, A.G. Marshall, Simultaneous Reduction and digestion of proteins with disulfide bonds for hydrogen/deuterium exchange monitored by mass spectrometry, Anal. Chem. 82 (2010) 1450–1454.
[86] L.M. Jones, H. Zhang, I. Vidavsky, M.L. Gross, Online, high-pressure digestion system for protein characterization by hydrogen/deuterium exchange and mass spectrometry, Anal. Chem. 82 (2010) 1171–1174.
[87] T.E. Wales, K.E. Fadgen, G.C. Gerhardt, J.R. Engen, High-speed and high-resolution UPLC separation at zero degree celsius, Anal. Chem. 80 (2008) 6815–6820.
[88] K.D. Rand, M. Zehl, O.N. Jensen, T.J.D. Jørgensen, Protein hydrogen exchange measured at single-residue resolution by electron transfer dissociation mass spectrometry, Anal. Chem. 81 (2009) 5577–5584.
[89] J. Pan, J. Han, C.H. Borchers, L. Konermann, Hydrogen/deuterium exchange mass spectrometry with top-down electron capture dissociation for characterizing structural transitions of a 17 kDa protein, J. Am. Chem. Soc. 131 (2009) 12801–12808.
[90] S. Faham, G.L. Boulting, E.A. Massey, S. Yohannan, D. Yang, J.U. Bowie, Crystallization of bacteriorhodopsin from bicelle formulations at room temperature, Protein Sci. 14 (2005) 836–840.